Advances in Aerospace Science and Applications.
ISSN 277-3223 Volume 10, Number 1 (2020), pp. 11-21
© Research India Publications
http://www.ripublication.com/aasa.htm

# Posthumous Analysis of the Indian Anti-Satellite Experiment Part II: Fragments Dispersion Study

**Arjun Tan[1]*, Robert C. Reynolds[2] and Rahul Ramachandran[3]**

*[1]Alabama A & M University, Normal, AL 35762, U.S.A.*

*[2]STAR Dynamics, Hilliard, OH 43026, U.S.A.*

*[3]National Space Science & Technology Center, Huntsville, AL 35806, U.S.A.*

**E-mail: arjun.tan@aamu.edu*

**Abstract**

The Indian anti-satellite (ASAT) experiment of 27 March 2019 created some unexpected results. Whereas the planned head-on impact of the ASAT with the target satellite was to minimize orbital debris production, the converse had actually happened. It has now been shown that a series of explosions within the target following the impact was responsible for the debris production. The magnitude, variance and directionality of the fragments produced in the primary explosion are analyzed in this study. It was found that 95% of the fragments were ejected in the forward direction, 69% were ejected in the downwards direction and 80% were ejected rightwards of the target when viewed from above. More than half of the fragments (58%) were ejected within just one octant of space (Octant VIII in the fragmenting satellite's local frame of reference). The angular distribution of the fragments was studied by defining angles of latitude and longitude at the breakup point and plotting them in an equidistant cylindrical projection map. The map clearly shows that the majority of the fragments were concentrated in a narrow solid angle within Octant VIII. The most energetic fragments located near the periphery of this octant strongly suggest that the target fragmented in a fashion similar to the 'Clam Model' of explosive fragmentation of propellant tanks.

## 1. INTRODUCTION

On 27 March 2019, ***India became the fourth nation in history to attain anti-satellite (ASAT) capability*** when its ***Microsat-R*** satellite was destroyed in Sun-synchronous orbit. The ASAT weapon was a ***kinetic kill vehicle*** (KKV) atop a third-stage rocket launched from Abdul Kalam Island [1]. The impact occurred at 11:13 IST or 05:43 UT on Julian day 2019086 which translates to epoch 2019086.23819444. The location

of the event was over Bay of Bengal at latitude 18.715$^{o}$N and longitude 87.450$^{o}$E [2]. This ASAT experiment was planned such that most of the fragments produced by the backward impulse would deorbit rapidly and pose no threat to the space environment. Actually however,the converse had happened. Several hundreds of fragments spread in the forward direction, many of them into higher orbits. This unexpected result has now been analyzed and explained in a recent study [3]. The results show that whereas collision alone was not responsible for the debris production, explosions resulting from the collision almost certainly created the hazardous orbital debris [3]. Careful examination of the '***Gabbard diagram***' showed that at least three secondary explosions following the primary one took place after the target satellite was knocked into an elliptical orbit as a result of the collision with the ASAT [3].

The magnitude, variance and directionality of the fragment velocities of a satellite breakup can shed valuable information regarding the nature and intensity of the breakup. For example, explosions are generally more efficient in fragments dispersion than collisions [4]. Moreover, the fragments dispersal from an explosion can be highly anisotropic depending upon the number of rupture sites [5]. In this paper, we report the fragments dispersion analysis of the Microsat-R breakup in orbit. Since the primary explosion of the target was from a nearly circular orbit [3], the fragmentation point was well-defined and the velocity perturbation calculations could be carried out without much uncertainty. However, the secondary explosions were from elliptical orbits with the remnant at locations having different true anomalies [3]. Hence, the velocity perturbations of the fragments from the secondary explosions could not be carried out without the exact locations of the breakup points and were thus not considered in this study.

## 2. METHOD OF ANALYSIS

It is convenient to calculate the velocity perturbations imparted to the fragments in the satellite's ***local inertial frame of reference*** at the point of the breakup [4]. In this coordinate system, the three orthogonal directions are defined by: (1) ***local vertical*** or ***radial direction*** from the center of the Earth *r*; (2) the ***local tangential direction*** in the plane of the orbit or the ***down-range direction****d*; and (3) the ***transverse direction*** along the orbital angular momentum vector of the satellite or the ***cross-range direction*** *x* [6]. In this coordinate system, the velocity $\vec{v}$ of the parent has the components ($v_r$, $v_d$, 0) where:

$$v_d = \frac{1}{r}\sqrt{\mu a\left(1-e^2\right)}, \qquad (1)$$

and

$$v_r = \pm\sqrt{v^2 - v_d^2}\ , \qquad (2)$$

and *a* is the ***semi major-axis*** and *e* the ***eccentricity*** of the parent's orbit; *r* is the radial distance from the center of the Earth; and $\mu$ is the ***gravitational parameter of the Earth***. In Eq. (2), the + sign corresponds to the ***ascending mode*** of the satellite (true

anomaly $\theta<\pi$) whereas the – sign corresponds to the ***descending mode*** ($\theta>\pi$). Upon fragmentation, the velocity of a fragment $\vec{v}' = \vec{v} + d\vec{v}$ has the components ($v_r + dv_r$, $v_d + dv_d$, $dv_x$) where:

$$dv_r = \pm\sqrt{\mu\left(\frac{2}{r} - \frac{1}{a'}\right) - \frac{\mu}{r^2}a'\left(1-e'^2\right)} - v_r\,, \qquad (3)$$

$$dv_d = \frac{\cos\xi}{r}\sqrt{\mu a'\left(1-e'^2\right)} - v_d\,, \qquad (4)$$

and

$$dv_x = \frac{\sin\xi}{r}\sqrt{\mu a'\left(1-e'^2\right)}\ . \qquad (5)$$

In Eq. (3), the + sign corresponds to the ***ascending mode of the fragment*** (***true anomaly*** $\theta'<\pi$), whereas the – sign corresponds to the ***descending mode*** ($\theta'>\pi$). The ***plane change angle*** $\xi$ can be expressed as a function of the ***inclinations*** $i$ and $i'$ of the parent's and fragment's orbits, respectively, and $\lambda$, the ***latitude of the breakup point*** [6]:

$$\xi = \pm\cos^{-1}\frac{\cos i\cos i' + \sqrt{\cos^2\lambda - \cos^2 i}\sqrt{\cos^2\lambda - \cos^2 i'}}{\cos^2\lambda}\ . \qquad (6)$$

The ***true anomaly*** $\theta'$ of the fragment at the time of the breakup, which dictates the sign of $v_r + dv_r$ in Eq. (6) is determined from the ***argument of latitude*** $u'$ and the ***argument of perigee*** $\omega'$ of the fragment at the time of the breakup [6]: $\theta' = u' - \omega'$. From the ***spherical triangle*** bounded by the meridian of the breakup point, the equator and the ground track of the satellite, one gets:

$$u' = \sin^{-1}\left(\frac{\sin\lambda}{\sin i'}\right), \qquad (7)$$

or,

$$u' = \pi - \sin^{-1}\left(\frac{\sin\lambda}{\sin i'}\right), \qquad (8)$$

for the ***northbound*** or ***southbound motion*** of the fragment, respectively [6].

Since the argument of perigee is perturbed by the ***oblateness of the Earth***, the argument of perigee of the fragment at the time of observation $\omega_0'$ is different from that at the time of fragmentation $\omega'$. From the rate precession of $\omega$, one gets [7]:

$$\omega' = \omega_0' - \frac{4.98\left(5\cos^2 i' - 1\right)dt}{\left(\frac{a'}{r_\oplus}\right)^{3.5}\left(1-e'^2\right)^2}, \qquad (9)$$

where $\omega$ and $\omega'$ are expressed in degrees and $dt$ is expressed in days.

In this study, we analyze the velocity perturbations of the primary explosion of Microsat-R from a nearly circular orbit [3]. The orbital elements data of the parent satellite and the fragments are taken from the ***space-track.org*** website [8], where the ***two-line orbital elements sets*** furnish the universal time, inclination, eccentricity, mean anomaly and mean motion of the parent satellite and the fragments.

## 3. VELOCITY PERTURBATIONS OF THE FRAGMENTS

**Table I.** Microsat-R Fragment Counts in Various Quarters of Space

| Regions of Space | $dv_d$ | $dv_x$ | $dv_r$ | Count | % of Total |
|---|---|---|---|---|---|
| Fragments in all space | all | all | all | 133 | 100.00 |
| Fragments ejected upwards | all | all | + | 41 | 30.83 |
| Fragments ejected downwards | all | all | − | 92 | 69.17 |
| Fragments ejected forwards | + | all | all | 126 | 94.74 |
| Fragments ejected backwards | − | all | all | 7 | 5.26 |
| Fragments ejected to the left* | all | + | all | 27 | 20.30 |
| Fragments ejected to the right* | all | − | all | 106 | 79.70 |
| Fragments ejected in Octant I | + | + | + | 15 | 11.28 |
| Fragments ejected in Octant II | − | + | + | 1 | 0.75 |
| Fragments ejected in Octant III | − | − | + | 0 | 0.00 |
| Fragments ejected in Octant IV | + | − | + | 23 | 19.29 |
| Fragments ejected in Octant V | + | + | − | 10 | 7.52 |
| Fragments ejected in Octant VI | − | + | − | 1 | 0.75 |
| Fragments ejected in Octant VII | − | − | − | 6 | 4.51 |
| Fragments ejected in Octant VIII | + | − | − | 77 | 57.89 |
| *Looking downwards from the parent satellite at fragmentation | | | | | |

Table I summarizes the fragments dispersion in various directions and quarters of space. Out of the 133 primary explosion fragments: ***31% were ejected upwards*** and ***69% were ejected downwards***; ***nearly 95% were ejected forwards*** and only ***5% were ejected backwards***; and nearly ***80% were ejected to the right*** when viewed from above. The last result meant that the ASAT had struck the target ***slightly from the west of a head-on collision***. Fragment counts in three-dimensional octants of space were highly selective. ***Nearly 58% (i.e. more than half) of the fragments were ejected within just one octant of space*** (Octant VIII in the target satellite's frame of reference) defined by $dv_d > 0$; $dv_x < 0$; and $dv_r < 0$.

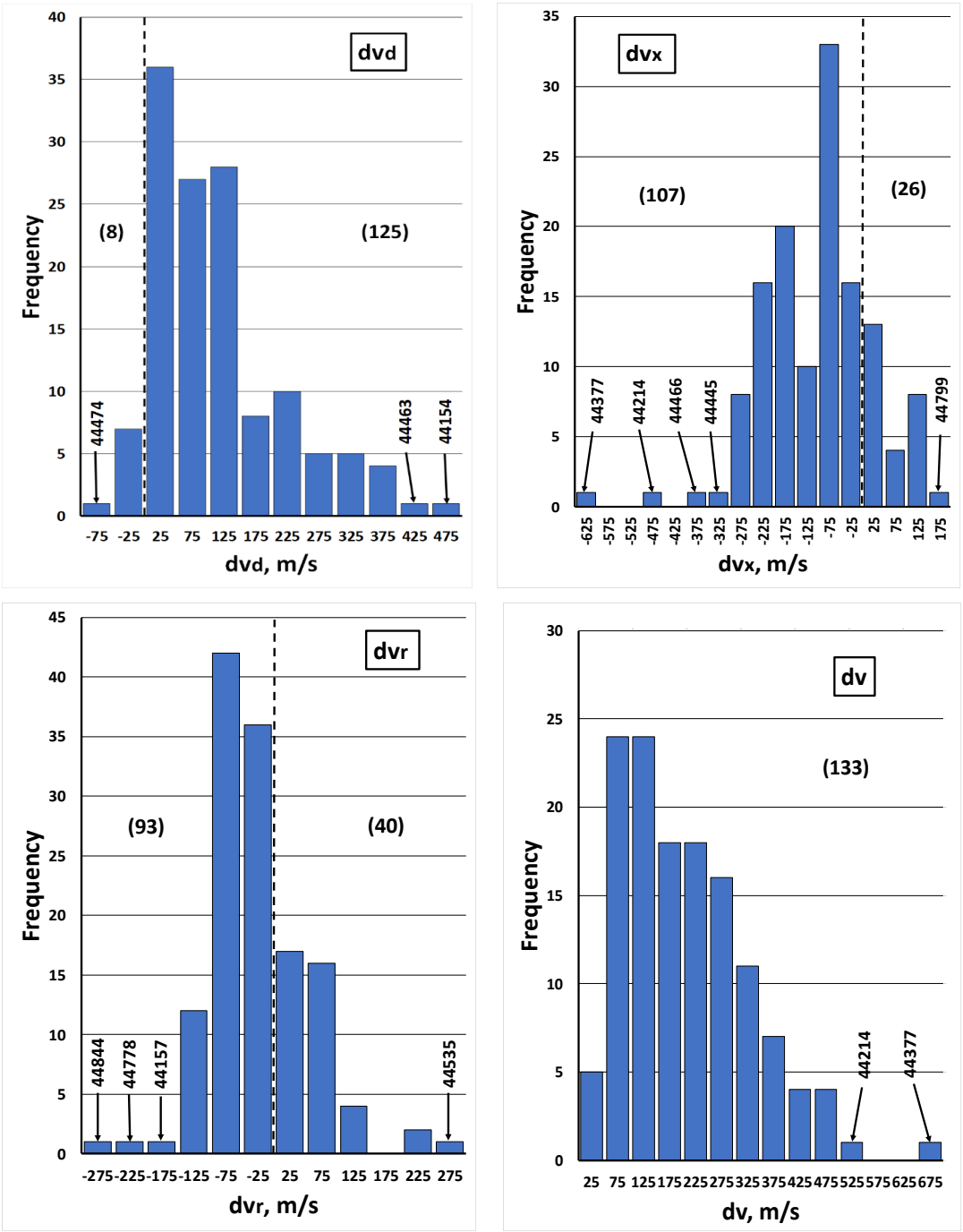


**Figure 1**

Figure 1 shows the frequency distributions of $dv_d$, $dv_x$ , $dv_r$ and $dv = \sqrt{dv_d^2 + dv_x^2 + dv_r^2}$. The $dv_d$ histogram was the ***most lop-sided*** and ***skewed to the right***; the $dv_x$ histogram had the ***greatest spread***; and the $dv_r$ histogram was the ***narrowest*** amongst the three. Fragments with extreme velocity perturbations are

marked in Fig. 1. Out of the 133 fragments, all except 8 were ejected in the forward direction, even though the kinetic impact from the ASAT was towards the backward direction of the target. This was the one of the first reasons to think that the fragments dispersion was due to the primary explosion that followed the collision. Granted, of course that fragments receiving large retrograde velocity perturbations were expected to have deorbited. The frequency distributions of $dv_x$ and $dv_r$ were more ***Gaussian*** than that of $dv_r$. Two fragments with the greatest velocity perturbations (fragments 44377 and 44214) were located outside the $dv_x$ Gaussian envelope. They were most likely to have originated from the impact area. The same two fragments also experienced the largest total ejection speeds $dv$. A vast majority of fragments were ejected to the right of the target's path when viewed from above, which meant that the ASAT struck the target slightly towards the left of the center. Interestingly, over two-thirds of the fragments were ejected downwards and still survived re-entry into the atmosphere. The $dv$ distribution exhibited a ***Maxwellian distribution pattern***.

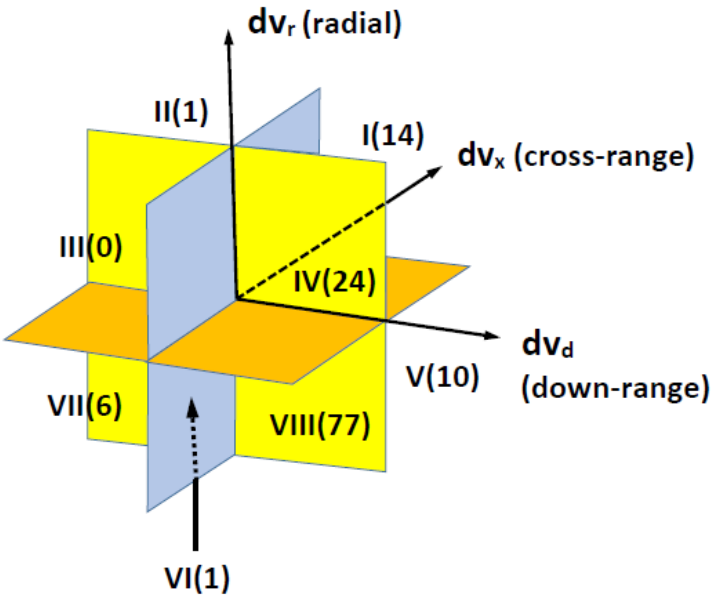


**Figure 2**

Figure 2 gives a ***three-dimensional perspective*** of the fragment counts of Table I. The fragment counts in the various octants of space are denoted in the target's frame of reference at breakup. Well over half of the fragments (77) were found in just one octant (Octant VIII). There was no fragment in Octant III and only one fragment each in Octants II and VI. That adds to only 8 fragments in the backward direction of the target's motion.

## 4. INCLINATIONS OF THE FRAGMENTS

Of the velocity perturbation components, it is the cross-range components $dv_x$ which is solely responsible for the change in inclination of a fragment from the fragmenting

parent in accordance with the equation [9]:

$$di = \frac{r\cos u}{na^2\sqrt{1-e^2}}dv_x \qquad (10)$$

where $n$ is the ***mean anomaly*** of the fragment. Thus the change in inclination is directly related to $dv_x$. Figure 3 is the frequency plot of the inclinations of the fragments of Microsat-R. It is no surprise that Fig. 3 closely resembles the frequency plot of $dv_x$ of Fig. 2. The original inclination of the parent is shown in the figure. Also marked are several fragments whose inclinations clearly fall outside the Gaussian envelope. As stated earlier, these fragment almost certainly originated from the contact area. Also, the inclination changes of the vast majority of the fragments were negative, which meant that their orbits became more northerly upon impact.

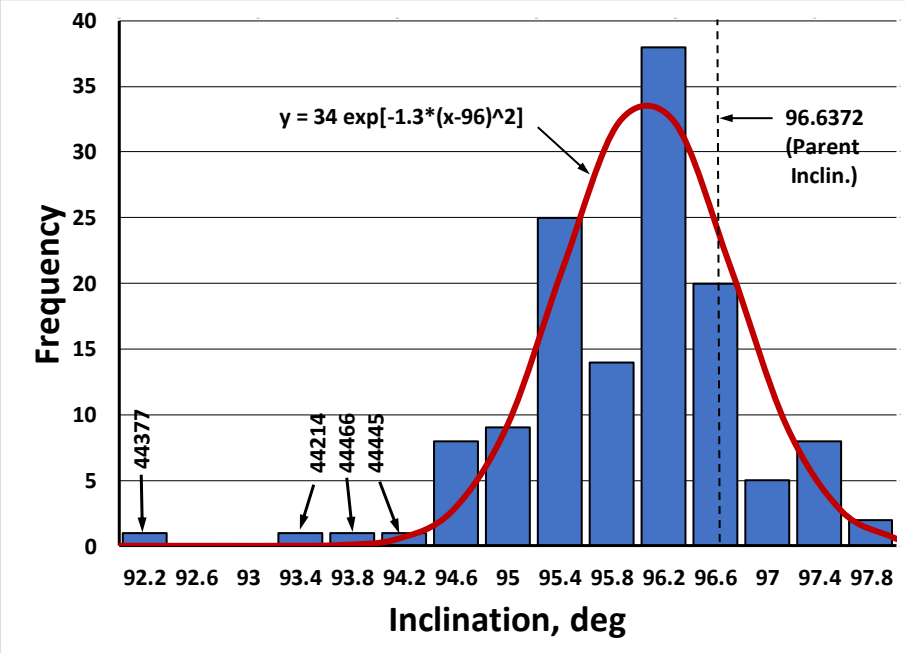


**Figure 3**

## 5. SCATTERPLOTS OF VELOCITY PERTURBATION COMPONENTS

Figure 4 is the ***scatterplot of the fragments*** in the ***horizontal*** $dv_d$-$dv_x$ ***plane*** (upper panel); and ***two vertical planes***: one containing the ***momentum of the parent satellite*** (lower left panel); and the other containing the ***angular momentum of the parent*** (lower right panel). Two fragments each with the greatest $dv_d$ and the greatest negative $dv_x$ are marked in the figure as are the directions of the target and the ASAT. The target satellite and the ASAT were in head-on collision when viewed from above (upper panel). The vast majority of the fragments were ejected forwards (126, Table I) and to the right (106) in the target satellite's frame of reference. The former points to

an ***explosive fragmentation***, whereas the latter indicates the role played by the collision in which the ***ASAT struck its target slightly to the left of the middle*** as seen from above. The two fragments with the greatest positive $dv_d$'s and the greatest negative $dv_x$'s emphasize this scenario.

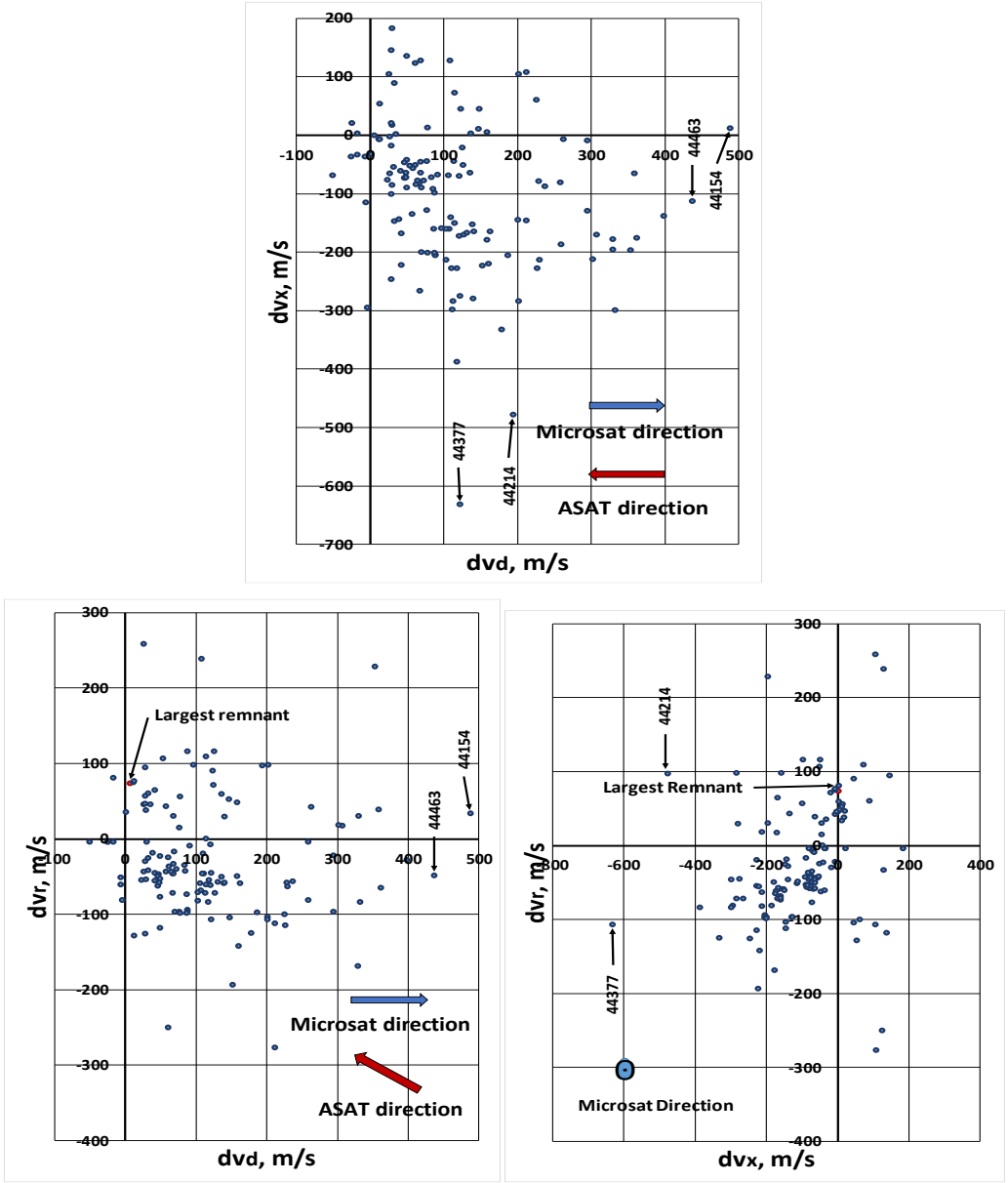


**Figure 4**

In the vertical plane containing the velocity of the target satellite (lower left panel of Fig. 4), more fragments (92, Table I) were actually ejected below the horizontal plane and still remained in orbit. Interestingly, ***most fragments actually went against the direction of the incoming ASAT***. This once again indicates the ***absence of a major role played by impact in this fragmentation***. It also points to the fact that most of the fragments (77, Table I) emerged in a ***narrow solid angle in the eighth octant of***

***space.***In the vertical plane looking into the target (lower right panel of Fig. 4), the majority of the fragments were ejected to the left below the horizontal plane. Both of the lower panel figures show the location of the ***largest remnant of Microsat-R*** which inherits the identity of the latter. Both figures indicate that this major fragment was boosted mainly in the vertically direction with a velocity perturbation of 74.44 m/s as a result of the impact with the ASAT. Consequently, its orbit became significantly elliptical. It would subsequently explode at least three more times to produce additional Gabbard diagrams within the Gabbard diagram of the primary explosion [3].

## 6. ANGULAR DISTRIBUTION OF THE FRAGMENTS

The angular distribution of the fragments studied by defining two angular coordinates: (1) the ***latitude*** $\lambda$, measured from the horizontal plane; and (2) the ***longitude*** $\phi$, measured from the plane of the orbit:

$$\lambda = \sin^{-1}\left(\frac{dv_r}{dv}\right), \qquad (11)$$

and

$$\phi = \tan^{-1}\left(\frac{dv_x}{dv_d}\right) + n\pi, \qquad (12)$$

where $n = 0$ if $dv_d > 0$; $n = 1$ if $dv_d < 0$ and $dv_x > 0$; and $n = -1$ if $dv_d < 0$ and $dv_x < 0$.

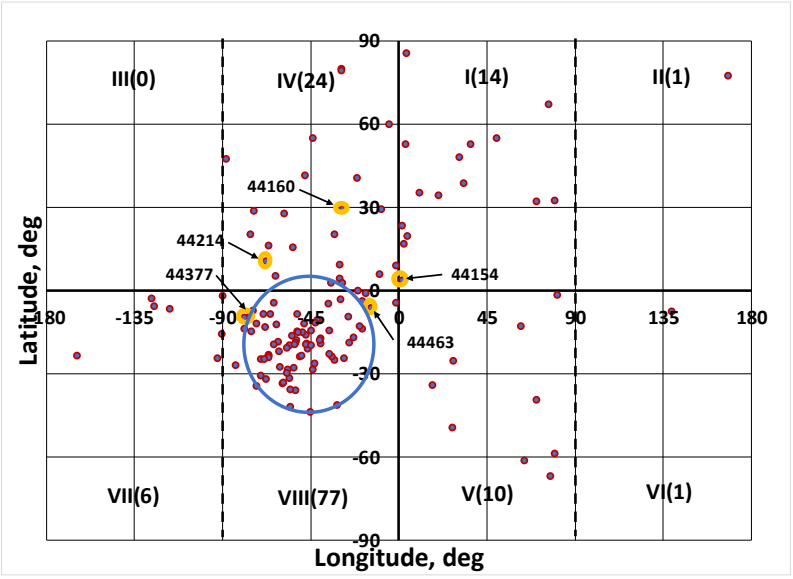


**Figure 5**

The angular coordinates of the fragments are plotted on an ***Equidistant Cylindrical Projection Map*** in Fig. 5. The octants of space are marked with their fragment counts on the map. As discussed in relation to Fig. 2, well over half of the fragments (77)

were found in just one octant (Octant VIII) and a vast majority of them were concentrated within a ***narrow solid angle marked by the oval*** in Fig. 5. Contrast to that no fragment was found in Octant III and only one fragment each was located in Octants II and VI. Incidentally, Octant II, largely devoid of fragments, lies diametrically opposite to Octant VIII having the largest number of fragments. Also marked in Fig. 5 are five fragments with the greatest velocity boosts *dv*. Interestingly they are located either just outside the oval in Octant VIII, or in Octant IV, which is adjacent to Octant VIII, i.e., they are all located near the periphery of the oval of concentration.

## 7. DISCUSSION

Following a string of Delta second-stage rocket explosions in orbit between 1973 and 1981, a model study of explosive fragmentation of propellant tanks was made using theory and computations [5]. According to this study, the fragment dispersion was highly anisotropic when there was a single rupture site. In this scenario called the ***Clam Model***, the gaseous products of the explosion escaped through the rupture site resulting in: (1) a few fragments in that direction; and (2) fragments with the greatest velocities ejected from the peripheral regions of the rupture site [5]. This scenario was shown to have been realized in the explosive fragmentation of the Nimbus-6 rocket in a recent study [10]. However, when applied to the Microsat-R fragmentation, the second aspect of the Clam model is realized, but not the first. In fact, the very opposite result happened: instead of a dearth of fragments, a majority of the fragments were ejected in the forward direction where the rupture was likely located. The reason for this lies in the fundamental difference in the structures of rockets and satellites: whereas rockets are basically hollow structures, satellites are densely packed with instruments. The escaping gases would carry fragments in front of them, especially if the gas tank is situated at the back of the satellite. Hence the Clam model applies differently to the breakup of rockets and satellites. In the case of the Microsat-R breakup, it may be said that ***the satellite likely fragmented in a fashion similar to the Clam model as applied to satellites***.

## REFERENCES

[1] https://wikipedia.org/wiki/Mission_Shakti.

[2] https://thediplomat.com/2019/05/why-indias-asat-test-was-reckless/.

[3] A. Tan, R.C. Reynolds & R. Ramachandran, Posthumous analysis of the Indian Anti-Satellite Experiment: Puzzles and Answers, *Adv. Aerospace Sci. Appl.*, *10*, 1 (2020).

[4] A. Tan, F. Allahdadi, S. Maethner& J. Winter, Satellite fragmentation: explosion vs. collision, *Orbital Debris Monitor*, *6*(*2*), 8 (1993).

[5] F.J. Benz, R.L. Kays, C.V. Bishop & M.B. Eck, *Explosive Fragmentation of Orbiting Propellant Tanks* in *Orbital Debris from Upper-Stage Breakup*, J.P. Loftus, Jr. ed., AIAA, Washington, 107-129 (1989).

[6] G.D. Badhwar, A. Tan & R.C. Reynolds, Velocity Perturbation Distributions in the Breakup of Artificial Satellites, *J. Spacecraft Rockets*, *27*, 299-305 (1990).

[7] D. King-Hele, *Theory of Satellite Orbits in an Atmosphere*, Butterworths, London (1964).

[8] https://www.space-track.org.

[9] L. Meirovitch, *Methods of Analytical Dynamics*, McGraw-Hill, New York (1970).

[10] A. Tan, A. Alomari& M. Schamschula, Analysis of the Nimbus-6 rocket fragmentation using theory and computations,*Adv. Aerospace Sci. Appl*., *7*, 25 (2017).